11. J. R. Melrose, D. B. Hibbert, and R. C. Ball, *Phys. Rev. Lett.*, **65,** 3009 (1990).
12. V. Fleury, J. Chazalviel, M. Rosso, and B. Sapoval, *J. Electroanal. Chem.*, **290,** 249 (1990).
13. M. Matsushita, M. Sano, Y. Hayakawa, H. Honjo, and Y. Sawada, *Phys. Rev. Lett.*, **53,** 286 (1984).
14. Y. Sawada, A. Dougherty, and J. P. Gollub, *ibid.*, **56,** 1260 (1986).
15. D. Grier, E. Ben-Jacob, R. Clarke, and L. M. Sander, *ibid.*, **56,** 1264 (1986).
16. D. Grier, D. A. Kessler, and L. M. Sander, *ibid.*, **59,** 2315 (1987).
17. D. Barkey, R. Muller, and C. Tobias, *This Journal*, **136,** 2199 (1989).
18. D. Barkey, R. Muller, and C. Tobias, *ibid.*, **136,** 2207 (1989).
19. P. Garik, J. Hetrick, B. Orr, D. Barkey, and E. Ben-Jacob, *Phys. Rev. Lett.*, **66,** 1606 (1991).
20. S. H. Davis, *J. Fluid Mech.*, **212,** 241 (1990).
21. F. R. McClarnon, R. H. Muller, and C. W. Tobias, *Ind. Eng. Chem. Fundam.*, **18,** 97 (1979).
22. J. Newman, *J. Phys. Chem.*, **73,** 1843 (1969).
23. D. D. Joseph, *European J. Mech. B/Fluids*, **9,** 565 (1990).
24. S. E. May and J. V. Maher, To be published.
25. D. W. DiFrancesco, Ph.D. Thesis, University of Pittsburgh (1990).
26. L. M. Sander, in "The Physics of Structure Formation," W. Guttinger and G. Dangelmayr, Editors, Springer-Verlag, Berlin (1987).
27. N. Ibl, *Electrochim. Acta*, **1,** 3 (1959).
28. D. G. Miller, J. A. Rard, L. B. Eppstein, and R. A. Robinson, *J. Solution Chem.*, **9,** 467 (1980).

Relation Between Plating Overpotential and Porosity of Thin Nickel Electrolytic Coatings

Chonglun Fan,[*,1] **J. P. Celis, and J. R. Roos**

Department of Metallurgy and Materials Engineering, Katholieke Universiteit Leuven, B-3001 Heverlee, Belgium

ABSTRACT

The relation between plating overpotential and porosity of thin nickel electrolytic coatings (0.2 μm) was investigated. The porosity of nickel coatings was shown to be dependent on coating structure, which is determined by the plating overpotential. A lower porosity can be achieved by using a relatively high plating overpotential resulting in the deposition of nickel coatings with fine grains. A relation between the through-coating porosity of thin nickel coatings and the activation overpotential was identified. At plating current densities approaching the limiting current density, the porosity tends to increase due to a mass transport effect on the coating thickness distribution along the substrate surface.

It is well known that the structure of electrodeposits and hence the structure-dependent coating porosity can be affected by the plating conditions (1). Pores in electrodeposits can be generated during either nucleation or growth stages. Most crystallites growing from nuclei coalesce perfectly but some do not (2). The gaps between these crystallites may be perpetuated at increasing coating thickness and result in the formation of pores (2). When the coalescing crystallites are misoriented with respect to each other, the coalescing boundaries are grain boundaries. Since the density of imperfections and the degree of disorder are higher at grain boundaries than anywhere else, most pores induced by a lack of coalescence would be situated at grain boundaries (3). Compared to the case of large grain size, a coating composed of fine grains is densely packed so that the pores generated at grain boundaries would be less (4). The coating porosity could therefore be associated with the grain size and related to plating overpotential, which is a dominant factor in controlling nucleation rate and crystalline growth during electrodeposition (5). However, hardly any information in this respect can be found in literature.

In the present study, the porosity of Watts nickel electrodeposits plated at different current densities on bronze substrates pretreated in different ways was measured by a coulometric test. The structure of the coatings was examined by transmission electron microscopy. The relationship between porosity of thin nickel electrodeposits, their grain size and the plating overpotential has been investigated.

In this paper, the term pore or porosity of coatings is referred to the through pores which extend from the substrate to the surface of the coating and leave some substrate area uncovered.

Experimental

The substrates used were rolled copper-tin sheets with a tin content of 6 weight percent (w/o). Before plating, the samples were either electropolished or mechanically ground.

After pretreatment, the samples with a plating area of 2.2 × 1.8 cm^2 were plated in a Watts bath containing 300 g/liter $NiSO_4 \cdot 6H_2O$, 50 g/liter $NiCl_2 \cdot 6H_2O$, 40 g/liter H_3BO_3 and 1 g/liter sodium lauryl sulfate used as wetting agent. In a galvanostatic mode, nominal plating current density was selected in a range from 0.5 to 14 A/dm^2, and the corresponding plating overpotentials were measured. The bath temperature was fixed at 55°C and pH at 3.4. A moderate agitation was achieved by using a magnetic stirrer at the bottom of a 500 ml plating beaker. The coating thickness was selected as 0.2 μm. The thickness measurement was carried out on polished cross sections.

The grain size of the coatings was examined with a JEOL 200 CX transmission electron microscope (TEM). The coatings investigated were 0.2 μm thick nickel foils stripped away from the electropolished bronze substrates by dissolving the substrate material in a chromic acid solution containing 500 g/liter CrO_3 and 28 ml/liter H_2SO_4 at 25°C.

A coulometric test (6) recently developed by the authors was used to assess the porosity of the thin nickel coatings. The test is based on a coulometric measurement performed during an anodic potentiodynamic polarization of the coated bronze substrates in a solution at 25°C containing 50 g/liter Na_2SO_4 and 1 g/liter Rochelle salt. During the polarization, the anodic current passing from the sample was integrated by a coulometer. The difference in electric charge recorded on a nickel-coated sample and on a pore-free coating of identical composition and surface area was used as a porosity index. The porosity indexes achieved are assumed to be proportional to the exposed substrate area on coated samples and allow for a quantitative determination and differentiation of the porosity in nickel

---

[*] Electrochemical Society Active Member.

[1] Present address: Département de Métallurgie et de Génie des Matériaux, Ecole Polytechnique, Montréal, Québec, Canada H3C 3A7.

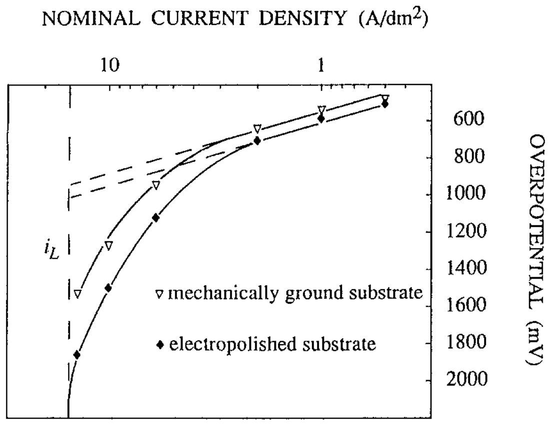

Fig. 1. Polarization for Watts nickel plating (55°C, pH 3.4) on either a mechanically ground or an electropolished substrate.

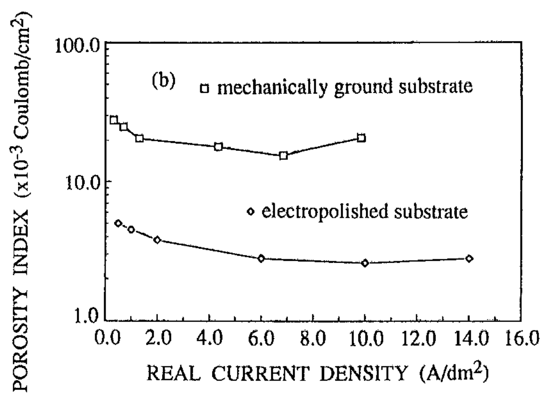

Fig. 2. Nickel porosity as a function of real plating current density on either mechanically ground or electropolished bronze (Watts bath, 55°C, pH 3.4, nickel thickness 0.2 μm).

coatings deposited on bronze. During the coulometric test, the anodic polarization was performed at a scan rate of 5 mV/s from 0.3 to 0.6 V *vs.* SCE. Two or three duplicate coulometric measurements were carried out for the coatings plated at an identical current density.

Results and Discussion

Figure 1 shows the cathodic overpotentials applied at different nickel plating current densities. At an identical plating overpotential on the same substrate material, the real plating current densities on both the electropolished and mechanically ground substrates would be equal. For the electropolished substrates, the surface is smooth; the real plated surface area enlarges little compared to the apparent surface area, and the real plating current densities can be supposed to equal the nominal plating current densities. For the mechanically ground substrates, however, the surface is rough; based on a comparison of the data on the polarization curves at identical plating overpotentials in Fig. 1, it can be revealed that the real plating current densities are only 1/1.4 of the nominal plating current densities. The porosity of 0.2 μm thick nickel coatings as a function of the real plating current density is shown in Fig. 2. The porosity decreases at increasing the real current density in a range below 7 A/dm² on mechanically ground substrates and below 10 A/dm² on electropolished substrates, and it increases as the real current density is increased beyond the ranges. Nickel coating plated on an electropolished substrate is apparently less porous than on a mechanically ground substrate.

At low cathodic overpotentials, it can be seen from Fig. 1 that the relationship between nickel plating overpotential and current density is linear in a semi log graph, as predicted by Tafel's law for activation-controlled electrodeposition. The Tafel lines in Fig. 1 follows the equations

$$\eta_a = 600 + 329 \log(i') \qquad [1]$$

for Watts nickel plating on the electropolished bronze, and

$$\eta_a = 556 + 329 \log(i') \qquad [2]$$

for Watts nickel plating on the mechanically ground substrates where η_a is the activation overpotential (mV); and i' the nominal plating current density (A · dm^{-2}). At sufficiently high overpotentials, Tafel's law holds no longer; a combined activation-transfer control stands for the plating. A limiting current density i_L for the Watts nickel plating of 15 A/dm² is measured from the nickel polarization on the electropolished substrate (see Fig. 1). The ratio of real plating current density to the limiting current density, i/i_L, is calculated for the nickel plating on both the electropolished and the mechanically ground substrates.

Dark field transmission electron micrographs of 0.2 μm thick nickel coatings plated at different current densities are shown in Fig. 3. A special feature of dark field images is that in contrast to bright field, only electron beams diffracted through crystals are observed. Areas of comparable brightness are indicative of grains having the same crystal orientation. The white areas in Fig. 3 allow the determination of the grain size and are not pores as would be the case if a bright field imaging mode had been used. A quantitative analysis of pore area by bright field TEM was not feasible. TEM specimens are very small and thus may not be representative of the whole coating unless a very large number of samples should be investigated. The grain size observed in the coatings is in the order of magnitude of 0.01 and 0.1 μm. The grain size decreases apparently at increasing plating overpotential.

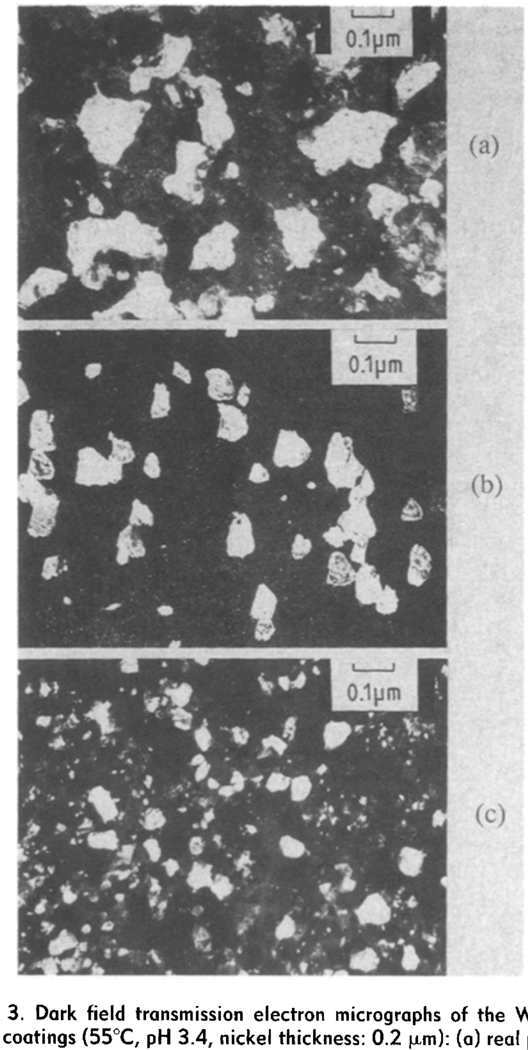

Fig. 3. Dark field transmission electron micrographs of the Watts nickel coatings (55°C, pH 3.4, nickel thickness: 0.2 μm): (a) real plating current density 0.5 A/dm², overpotential 508 mV; (b) real plating current density 6 A/dm², overpotential 1123 mV; and (c) real plating current density 14 A/dm², overpotential 1860 mV.

Mechanisms involving nucleation have been frequently invoked in the description of metal electrodeposition theory. At a sufficiently high rate of electrodeposition, if the rate control is such that the adion concentration increases with increasing potential, the probability of nucleation is high. A mathematical equation was established by Bockris and Damjanovic (5) showing that the critical radius of a nucleus (for simplicity assumed to be circular) in an electrodeposit is inversely proportional to the logarithm of an adion concentration ratio

$$r_c = \frac{3^{1/2} d^2 \gamma}{2kT \ln (c/c_0)} \qquad [3]$$

where r_c is the critical radius of a nucleus (cm), d the interatomic distance in the nucleus (cm), γ the edge energy in unit length of the circumference of the nucleus ($J \cdot cm^{-1}$), k the Boltzmann constant ($J \cdot K^{-1}$), T absolute temperature (K), c and c_0 the adion concentration at the electrode surface ($mole \cdot cm^{-2}$), respectively, at a given overpotential and at zero overpotential. In Eq. [3], the factor $3^{1/2}/2$ accounts for the close packing of atoms in the embryo on the (111) plane of fcc metals. Since the activation energy for transfer from a hydrated ion in solution to an uncharged species on the electrode is too large to allow for appreciable transfer rates, the transferred particle is an adion and not an adatom (5). If the electrodeposited surface is considered as crystallographically flat, a growth step-free surface, after the application of a constant cathodic overpotential across the electrical double layers at the electrode surface, the adion concentration on the deposited surface in the steady state can be derived (7)

$$c = c_0 \exp\left(\frac{ZF\eta_a}{1000RT}\right) \qquad [4]$$

where Z is the number of charges involved in the electrochemical reaction, F the Faraday constant ($C \cdot mol^{-1}$), η_a the cathodic activation overpotential during plating (mV), and R the gas constant ($J \cdot mol^{-1} \cdot K^{-1}$). The equation indicates that the adion concentration c is strongly dependent on the applied cathodic overpotential on the electrode surface. Under the condition that the activation at the cathode-solution interface is the step-controlling reaction for electrodeposition, the applied cathodic overpotential η is purely composed of the activation overpotential η_a and follows Tafel's law (see Fig. 1). As the cathodic overpotential increases beyond the activation range, the applied overpotential η contains then two portions (8): the activation overpotential η_a and the concentration overpotential η_c. The activation overpotential η_a can be derived from an extrapolated Tafel line (see Fig. 1).

Based on Eq. [4], the adion concentration ratio in Eq. [3] can be then replaced by an exponential function of the cathodic activation overpotential, one has

$$r_c = \frac{10^3 3^{1/2} d^2 \gamma N_A}{2ZF\eta_a} \qquad [5]$$

where N_A is the Avogadro number (mol^{-1}).

In electrodeposition, increasing the cathodic overpotential of the electrode can result in a higher electrical field at the interface between the cathode surface and the solution. When this is the case, more metal ions (with positive sign) should be adsorbed onto the cathode surface, and the corresponding adion concentration c would be increased (Eq. [4]), and the critical radius of nuclei decreases (Eq. [5]). For a given thickness of coating material, fine grains in a coating indicate that the number of crystallites and the rate of nucleation during plating are relatively high. As Bockris and Damjanovic (5) derived, the nucleation rate (the number of embryos per cm^2 becoming nuclei in 1 s) increases with decreasing critical radius of nuclei. Therefore, fine grains in a coating can be related to small critical radius of nuclei and high plating overpotential. This is in accordance with the experimental results achieved in this work. Compared to the case of large grain size, a coating composed of fine grains would be less porous. In the present work, for thin nickel coatings plated at a current density well below the limiting current density ($i/i_L < 0.6$ for plating on the mechanically ground bronze, and $i/i_L < 0.9$ for plating on the electropolished bronze), the coating porosity decreases with decreasing grain size in the coatings, which is achieved by increasing the plating overpotential. Since a low porosity is related to fine grains and the grain size decreases with decreasing critical radius of nuclei, the low porosity of thin nickel coatings may further correspond to a small critical radius of nuclei. If the porosity of thin nickel electrodeposits is supposed to follow a linear relationship with the critical radius of the nuclei in electrodeposition, one should have

$$p = m r_c \qquad [6]$$

where p is the coating porosity, in this work the porosity index ($C \cdot cm^{-2}$), and $m \geq 0$, a proportionality constant ($C \cdot cm^{-3}$).

Combining Eq. [5] and [6], one has

$$p = \frac{B}{\eta_a} \qquad [7]$$

where $B = (m 10^3 3^{1/2} d^2 \delta N_A)/(2ZF)$ is a constant in the experimental conditions and has a dimension of $C \cdot mV \cdot cm^{-2}$ for η_a in millivolts.

To verify this proposed relationship between nickel porosity and plating overpotential, the experimental data obtained for the 0.2 μm thick Watts nickel coatings plated at nominal current densities lower than or equal to 10 A/dm² have been used. Based on the porosity indexes and the corresponding activation overpotentials and by using the method of least squares, the constant B in Eq. [7] was determined: 2.6 and 13.6 $C \cdot mV \cdot cm^{-2}$ for the coatings plated on the electropolished and mechanically ground substrates (see Fig. 4).

The constant B in Eq. [7] is composed of structural parameters of the coating material (d, γ, and Z) and the proportionality factor relating the porosity index to the critical radius of nuclei (m). It is expected that the structural parameters and the proportionality factor vary with different coating materials, plating, and substrate conditions. In this work, with the identical bath composition and plating conditions, the structural parameters of nickel coatings plated on same substrate material could be unchanged. The difference in the value of B for thin nickel coatings plated on electropolished and mechanically ground substrates could be attributed to the difference in the proportionality factor in the case of different substrate conditions. Under identical electrochemical conditions, with same critical radius of nuclei, the porosity of thin Watts nickel coatings plated on mechanically ground substrates is higher than on electropolished substrates. Therefore, the constant B in Eq. [7] and the porosity proportionality factor m are dependent on substrate conditions.

The proposed relation between nickel porosity and plating overpotential (Eq. [7]) can only be applied to the case that an electrodeposition is carried out at a current density well below the limiting current density on the mechanically ground bronze ($i/i_L < 0.6$). As the cathodic overpotential is increased further, eventually the limiting current density (i_L) will be approached, and the porosity of nickel coatings increases (see Fig. 2 and 4). Besides the structural effect, other effects should be then taken into account. When the plating current density is increased close to the limiting current density, the rate of metal deposition is mainly controlled by the mass transport of the cations toward the cathode and the mass transport is then the main factor governing the current density distribution. The mass transport effect on the distribution of plating current density and coating thickness on an electrode surface depends on a comparison of substrate surface roughness and the thickness of the diffusion layer at the electrode surface. As the diffusion layer is much thicker than substrate roughness, the distribution of plating current density and coating thickness cannot be uniform on the coated electrode surface (9). As our previous work has shown (6), the porosity of thin nickel electrodeposits increases at de-

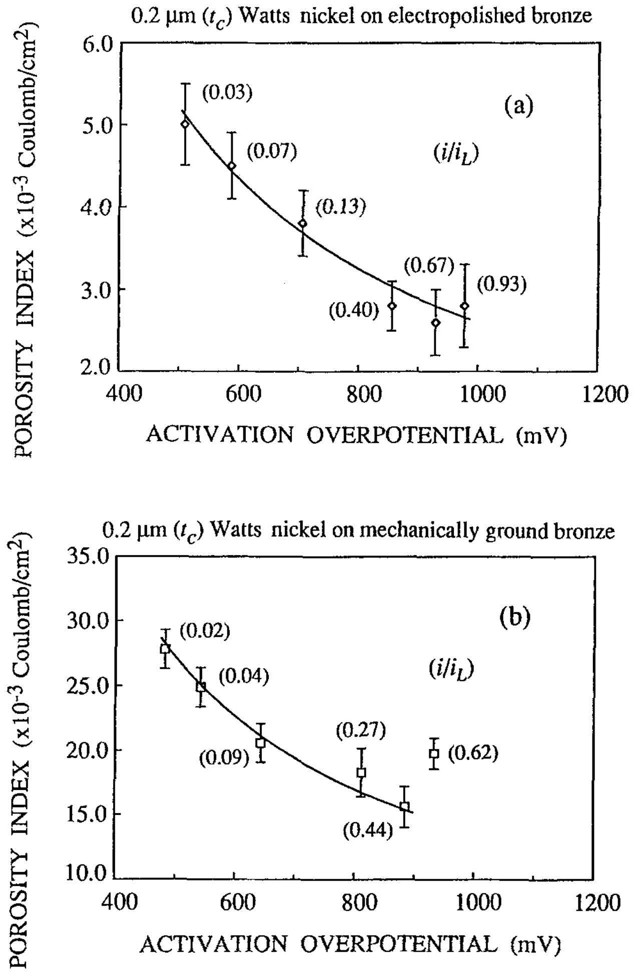

Fig. 4. Porosity index of 0.2 μm thick Watts nickel coatings vs. activation overpotential in plating: (a) on electropolished bronze and (b) on mechanically ground bronze.

creasing coating thickness, and the porosity is most strongly dependent on the thinner parts of a coating. If the coating thickness is not uniform on an electrode surface, the porosity will be more pronounced compared to the case that a uniform thickness distribution can be achieved with a same average coating thickness. The extra porosity arises from the thinner parts of the coating. Under the experimental conditions in this work, the diffusion layer at the electrode surface should be much thicker than 10 μm (8, 9) and much thicker than the surface roughness of the substrates. Therefore, at a plating current density approaching the limiting one, the uniformity of the coating thickness distribution on the electrode surface would be diminished (see Fig. 5). This overcomes the effect of high plating overpotential to reduce the porosity and results in the tendency to increase the porosity of coatings. The roughness of the electropolished substrates is close to zero, and the geometric variation between asperities and recesses at the electrode surface is limited. The difference in the access for diffusion at the asperities and recesses is therefore rather small, and then the deterioration of the uniform distribution of plating current density and coating thickness caused by mass transport is not severe.

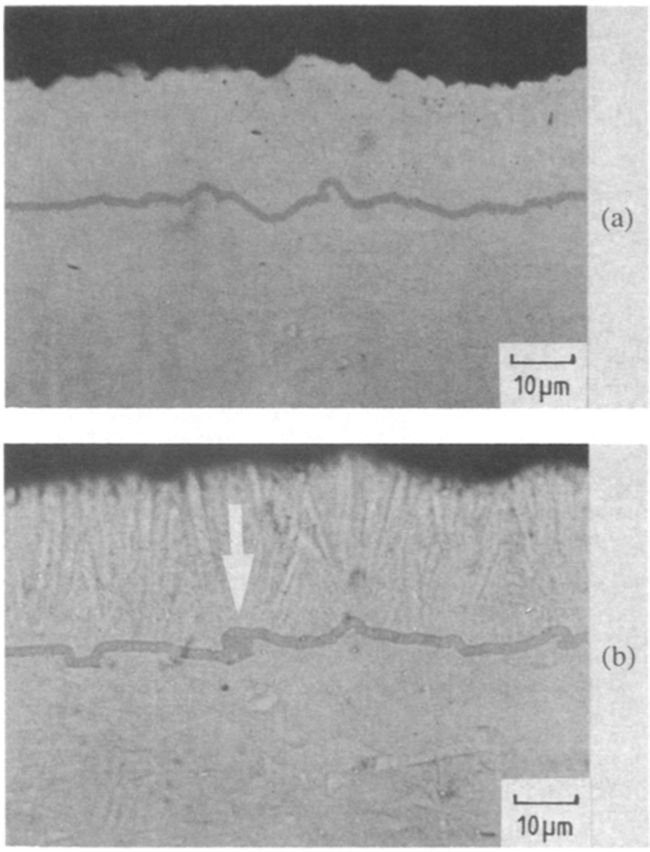

Fig. 5. Cross section of nickel coatings (Watts bath, 55°C, pH 3.4) on mechanically ground bronze: (a) uniform coating thickness, nominal plating current density 6 A/dm^2 (i/i_L: 0.27) and (b) an area of somewhat thicker coating, nominal plating current density 14 A/dm^2 (i/i_L: 0.62).

Conclusions

The porosity of nickel coatings is dependent on coating structure and is related to plating overpotential which determines structural characteristics of the coatings. In the case of nickel plating carried out well below the limiting current density ($i/i_L < 0.6$ for plating on the mechanically ground bronze and $i/i_L < 0.9$ for plating on the electropolished bronze), a lower porosity in nickel electrodeposits with a small grain size can be obtained by using a relatively high plating overpotential. The relation between the porosity of thin Watts nickel and the activation overpotential in plating can be quantitatively described. However, for the plating current density approaching the limiting current density, the nickel porosity tends to increase. This can be related to the mass-transport effect on the coating thickness distribution on the substrate surface.

Manuscript submitted Nov. 1, 1990; revised manuscript received April 20, 1991.

Katholieke Universiteit Leuven assisted in meeting the publication costs of this article.

REFERENCES

1. J. M. Leeds, *Trans. Inst. Metal Fin.*, **47**, 222 (1969).
2. M. Clarke, *ibid.*, **51**, 150 (1973).
3. S. Nakahara, *Thin Solid Films*, **45**, 421 (1977).
4. D. L. Rehrig, *Plating*, **61**, 43 (1974).
5. J. O'M. Bockris and A. Damjanovic, "Modern Aspects of Electrochemistry," Vol. 3, pp.224-346, J. O'M. Bockris and B. E. Conway, Editors, Butterworths, London (1964).
6. J. R. Roos, J. P. Celis, and Chonglun Fan, *This Journal*, **137**, 1096 (1990).
7. A. Damjanovic and J. O'M. Bockris, *ibid.*, **110**, 1035 (1963).
8. J. O'M. Bockris and A. K. N. Reddy, "Modern Electrochemistry," Vol. 2, pp. 845-1139, A Plenum/Rosetta Edition, New York (1977).
9. N. Ibl, *Surf. Technol.*, **10**, 81 (1980).